AD693361

ERDE 1/S/69

MINISTRY OF TECHNOLOGY

EXPLOSIVES RESEARCH AND DEVELOPMENT ESTABLISHMENT

SURVEY No. 1/S/69

Forced Convection Heat Transfer to Supercritical Cryogenic Hydrogen : Part 1 : Literature Survey

J.C. Beech

WALTHAM ABBEY
ESSEX

H5

ERDE 1/S/69 WAC/190/05

MINISTRY OF TECHNOLOGY

EXPLOSIVES RESEARCH AND DEVELOPMENT ESTABLISHMENT

SURVEY No. 1/S/69

Forced Convection Heat Transfer to Supercritical Cryogenic Hydrogen: Part 1: Literature Survey

by

J.C. Beech

Approved:	H. ZIEBLAND SCE
Approved for Circulation:	G.H.S. YOUNG PS/D

28th February 1969

WALTHAM ABBEY
ESSEX

Further copies of this survey can be obtained from Mintech, TIL, Block 'A', Station Square, St. Mary Cray, Orpington, Kent. BR5 3RE

FOREWORD

Analytical studies on the optimum propellant combinations for large multi-stage rockets have clearly indicated the superiority of liquid hydrogen as fuel for the upper stage propulsion units.

Lack of experience and technical know-how, largely the absence of efficient and sufficiently reliable ancillary equipment, such as tanks, pumps, valves, control equipment, etc., inhibited the use of hydrogen in the first generation of ELDO vehicles.

To fill this gap, various research programmes were launched in this country about 4 years ago at ERDE, RPE and RAE, with the objective to gather fundamental data and technological information on various aspects connected with the hydrogen/oxygen propulsion system.

This Establishment undertook to carry out extensive heat transfer studies with liquid hydrogen in its liquid and near-critical fluid phases. In order to make the results directly applicable to the requirements of the design engineers, test sections were developed having the shape and size of cooling channels likely to be used in a second-stage propulsion unit of a three-stage rocket vehicle.

Extensive preparatory studies and surveys leading to the design and construction of a complex test rig were undertaken during 1966 and 1967. However, shortly before the actual commencement of experiments with liquid hydrogen, the change in this country's space research policy resulted in the cancellation of almost all work involving liquid hydrogen for rocket propulsion, and consequently in the abandonment of this projected research.

The work involved the full-time effort of several members of the staff at ERDE for over 2 years, and considerable material expense. It was thought desirable, therefore, to record the status attained in detail, should it be decided to take up this work again at some future date.

In the first part, an extensive survey of all known published information on the subject of heat transfer to fluid hydrogen at supercritical pressures is presented; in the second part, the aims of the projected research are discussed and a comprehensive description of the design details of the apparatus and its associated equipment are given, including the proposed operating procedures and safety features of the test rig.

H. Ziebland
SCE

CONTENTS

SUMMARY

The published experimental data covering forced convection heat transfer to cryogenic hydrogen are reviewed, with special attention to the near-critical regions of temperature and pressure. Data for straight and curved tubes, of both circular and non-circular cross-sections, are covered; also the case of asymmetric peripheral heat flux through the walls.

A number of theoretical and semi-empirical treatments of the near-critical, variable fluid property condition are discussed, and their effectiveness in correlation of near-critical heat transfer to cryogenic hydrogen considered.

Reference: WAC/190/05

1. INTRODUCTION

The feasibility of using hydrogen under supercritical conditions as a regenerative rocket coolant has been established, both by experiment and by computation (1) based on a knowledge of the physical properties over the range of likely operating conditions, including cryogenic temperatures.

Experiences of hydrogen rocket design in the USA suggest that the behaviour of hydrogen as a coolant is more difficult to predict using the conventional forced-convection correlations, and allowing for the variations of fluid properties with temperature and pressure, than that of most fluid coolants.

Hydrogen is an unusual regenerative coolant in that it is possible for the fluid, while at supercritical pressures, to be heated from subcritical bulk temperatures (since storage may be at temperatures close to the normal boiling point at 20°K), through its critical temperature (33°K) during passage through the coolant channels.

At some locations in the coolant passages, therefore, the bulk fluid temperature will attain values in the region above the critical point, in which the physical properties of the fluid are very strongly temperature dependent and the specific heat (C_p) and Prandtl Number show marked peaks on individual isobars for pressures immediately above the critical pressure.

It is therefore necessary to determine how the convective heat transfer processes, and in practice heat transfer coefficients, differ from those adequately represented by the well-established constant property correlations; and desirable to provide a means of reliably estimating heat transfer in actual cooling channels of rocket engines designed to operate under these conditions.

As a consequence of operating in the critical region of temperature and pressure, large changes in fluid density will occur along some sections of the coolant tubes, and these must also be estimated reliably for design purposes, to ensure that excessive momentum pressure drops do not occur.

It should be emphasised that these unusual property variations and the associated transfer phenomena, are confined to a rather narrow range of pressure above the critical pressure. In rocket engines where combustion occurs at highly supercritical pressures ($P/P_c >> 5$) these conditions will not arise, and for practical purposes the fluid can be considered, above a certain temperature, to have monotonically varying properties.

2. PROPERTY VARIATIONS IN THE NEAR-CRITICAL REGION

In a number of technological applications, severe physical-property gradients (both radial or axial) may occur, making unreliable the use of empirical correlations or theoretical analyses based on the constant property conditions. These property gradients are most usually associated with gradients of temperature, or high ratios of wall temperature to fluid bulk temperature, since all the relevant physical properties of fluids are to some extent temperature dependent.

/A familiar .....

A familiar example of this is the modification to the forced convection correlation

$$Nu = f\ (Re,\ Pr) \qquad \ldots\ldots\ \underline{1}$$

made by Sieder and Tate (2) to account for the effect of the large difference in viscosity between the bulk fluid and that at the wall when heating or cooling viscous liquids, finding wide application, for example, in commercial tube and shell heat exchangers:

$$Nu_b = f\left(Re_b,\ Pr_b,\ \frac{\mu_b}{\mu_s}\right) \qquad \ldots\ldots\ \underline{2}$$

In flow of gases at supersonic velocities, extreme wall- to bulk fluid-temperature ratios are encountered, and fluid properties vary greatly between the cooled wall and the fluid stream. In allowing for the variation of properties, e.g. across the fluid stream cross-section, it is often possible to express the individual transport and thermal properties as simple linear functions of temperature, since their variation is monotonic with temperature. A similar condition may occur in cases where heat is transferred at very high heat fluxes to liquids.

The region in which pressure is greater than the critical pressure of the fluid, while the temperature may be close to, but below or above the critical temperature, is referred to here as the "supercritical region". Of special interest is the region of pressure above the critical pressure, up to reduced pressure of approximately 2, where small changes in either temperature or pressure can lead to drastic changes in the magnitude of fluid properties. This region is referred to herein as the "near-critical" region.

The most striking variation with temperature occurs in the specific heat at constant pressure, which at the critical point has infinite value. Above the critical pressure, the C_p isobars each have a pronounced maximum close to the critical temperature. The temperature at which this maximum value occurs on a particular supercritical isobar, referred to as the "transposed critical temperature" at that pressure, increases with pressure, the value of the maximum specific heat declining steadily with increasing pressure.

In general other physical properties of the fluid show their maximum rate of change with temperature near the transposed critical temperature. Measurements of the thermal conductivity of carbon dioxide (3) and ammonia (4) close to the critical point have shown that marked peaks occur in this region. Evidence suggests that the maxima are less strong and attenuate more rapidly away from the critical point than those of the specific heat, C_p. The maxima in both C_p and thermal conductivity appear to occur in fluid at the critical density.

/2.1 .....

2.1 Boiling-like Phenomena in the Near-critical Region

In spite of these drastic property variations in the near-critical region, the fluid is usually considered to be a monophase, although it cannot be considered wholly gaseous or liquid. It is, however, possible to consider the existence of two quasi-phases above the critical pressure, under transient, non-equilibrium conditions, which could occur during transfer of heat to the fluid. By an examination of the variation of, for example, density, viscosity, thermal conductivity and specific heat of the fluid in the near-critical region, it can be seen that the transposed critical temperature represents a point of transition from the type of property characteristics occurring at relatively low temperatures, to that typical of higher temperatures.

The fluid at temperatures well below the transposed critical temperature exhibits typical liquid property characteristics: the specific volume variation indicates a low value of thermal expansion coefficient; viscosity (μ) and thermal conductivity (k) are high, decreasing markedly with temperature. At temperatures considerably above the transposed critical temperature, conductivity, viscosity and density all have the relatively low values typical of gases; μ and k also increase slightly with temperature and the fluid density is inversely proportional to the absolute temperature.

From these considerations, Goldmann (5) postulated a mechanism of heat transfer in supercritical fluids, rather similar to nucleate boiling and based on the difference in physical properties between the dense fluid comprising the bulk of the fluid stream, and the "gas-like" fluid close to the wall at a much higher temperature. There is experimental evidence, obtained with a number of fluids, that some such mechanism occurs:

(i) peaks in the local heat transfer coefficient distribution, related to surface temperatures (or in some cases the "film" temperature) close to the transposed critical temperature (6,7),

(ii) photographic evidence that a separation of pseudo-phases occurs at supercritical pressures in pool boiling experiments (8), and

(iii) observations of severe vibrations or oscillations in this region, in forced convection flow systems and natural circulation loops, for hydrogen (9). and for other fluids (5,10,11). In many cases these effects have been recorded simultaneously with large increases in measured heat transfer rates without corresponding increase in the wall temperatures, a familiar phenomenon with nucleate boiling in flow systems.

Other experimenters have not observed the above phenomena associated with "boiling-like" behaviour. Rather the property variations of the near-critical region have been manifested in unusual axial wall temperature distributions (12); in distinct minima in local heat transfer coefficients, associated with the local bulk fluid temperature (13,14,15); and in distorted temperature and velocity profiles across the flow cross-sections (16). In a number of these studies in the critical region it was observed that under certain conditions, heat transfer coefficients declined consistently with increasing heat flux, e.g. Reference 6, as is predicted by the theoretical treatment of Deissler (17).

/The ....

The occurrence of "boiling-like" mechanism is evidently dependent on the local values of bulk fluid and surface temperatures, and their relation to the transposed critical temperature.

In general, for those cases where surface temperatures of the same order as the critical temperature were attained, but the bulk fluid was much below this temperature, phenomena similar to nucleate boiling were reported.

In the other group of experiments, in which bulk fluid temperatures close to the transposed critical temperature were encountered, the occurrence of maxima or minima in the local values of heat transfer coefficients was related to the magnitude of the temperature difference between the heated surface and the fluid. At very high temperature differences, minimum values of heat transfer coefficient occurred when the bulk temperature was close to the critical temperature. At lower temperature differences, the local heat transfer coefficient showed a maximum value under these conditions. This influence of temperature difference suggests a further analogy with boiling phenomena. Nucleate boiling, occurring at low temperature differences, sustains high rates of heat transfer, but at much higher temperature differences is superseded by film boiling where the insulation of the hot surface by an unbroken vapour film allows only much reduced rates of heat transfer to the bulk of the liquid.

There is strong experimental evidence that buoyancy forces become important in heat transfer at near-critical conditions, and may account for a number of the phenomena described above. This is particularly the case when local peaks in surface temperature occur at locations where the bulk fluid is close to the transposed critical temperature. Under these conditions the orientation of the tube, and also the direction of flow in vertical tubes, may clearly indicate the influence of buoyancy forces.

Shitsman (18) investigated the occurrence of peaks in the local surface temperature in the flow of near-critical water in vertical tubes, and showed that when the flow was downwards, i.e. when the buoyancy forces were opposed to the forces associated with the forced flow, the peaks did not occur. This is shown in Fig. 1, which is reproduced from Reference 18; this also shows that the surface temperature profiles for upward flow had the anomalous peaks above a certain heat flux, although the experimental conditions were otherwise similar.

Miropolskiy et al. (19) also reported the occurrence of anomalous peaks in the wall temperature for upward flow of near-critical water, as shown by curve 3 of Fig. 2. Curves 1 and 2 of this figure also indicate that the surface temperature profile may be significantly different at the top and bottom of a horizontal tube.

In this connection may be mentioned some high-speed photographic studies made in this Laboratory of heat transfer from electrically heated rods to kerosine flowing in a rectangular cross-section channel. These confirm that buoyancy effects are also important for the case where $T_s > T_m >> T_b$. These observations were made at a reduced pressure of approximately 1.5, with bulk temperatures near ambient, and surface temperatures somewhat above the estimated critical temperature for the fluid (398°C).

/It .....

It was observed that with turbulent flow of near-critical fluid, the violent activity at the surface was predominantly at the top of the rod, this effect becoming more marked as the flow rate was reduced. At Reynolds number of approximately 2000 (taking the rod diameter as characteristic dimension) good ciné films were obtained at up to 4500 frames per second. Very violent activity was observed to occur at the top surface only, causing turbulent density changes well into the bulk of the stream, whereas at the lower surface there was virtually no activity. This can be seen in Fig. 3, which is reproduced from one frame of the relevant ciné film.

For the case of flows through vertical tubes, Brown and Gauvin (20,21), in studies of temperature and velocity fluctuations in air flowing at Reynolds numbers between 270 and 6900, have demonstrated that turbulent transport depends on the interaction of free and forced convection. The magnitude of turbulent heat transfer is determined by the temperature and radial velocity fluctuations in the fluid stream, and the correlation coefficient between them. In upward flow the effect of buoyancy is to reduce the correlation coefficient, and so impair the effectiveness of the radial turbulent fluctuations in the transfer of heat.

Similarly, in near-critical heat transfer, the buoyancy forces in forced upward flow can produce local "laminarisation" of the flow, which is manifested as a peak in the wall temperature.

/TABLE 1 .....

TABLE 1

Experimental Data: Ranges of Variables for Supercritical Cryoge
Straight Circular Tubes

Authors		Ranges of Reduced Variables			Ratio T_s/T_b	Max He Fl (cal/c
		Pressure	Bulk Fluid Temperature (T_b)	Surface Temperature (T_s)		
Szetela	(50)	1.13 and 1.68	1.25 to 1.44	3.6 to 13.2	2.9 to 10.2	[illegible]
Miller et al.	(25)	2.1 to 13.2	0.86 to 3.1	-	-	9.
Thompson and Geery	(15)	3.6 to 7.1	0.91 to 1.73	30.5 (Max)	16.5 (Max)	3
Core et al.	(22)	1.0 to 1.13	0.93 to 2.5	25.0 (Max)	6.3 (Max)	2.
Perroud et al.	(30)	1.0 to 1.25	0.76	24.0 (Max)	-	[illegible]
Hendricks et al.	(33)	1.17 to 2.8	0.9 to 5.3	-	-	[illegible]
Hendricks et al.	(31)	1.2 to 4.2	0.66 to 2.0	-	13.0 (Max)	[illegible]
Wright and Walters	(23)	approx 3.7	1.6 to 2.3	-	-	[illegible]
Hendricks, Simoneau and Friedman	(34)	5.3 to 13.3	1.0 to 3.3	2.4 to 20.0	11.0 (Max)	2
Aerojet	(37)	3.7 to 7.3	1.0 to 1.6	7.2 to 28.0	-	8

*These references do not state the tube orientation explicitly, t
given here being deduced from figures or schematic diagrams

A

TABLE 1

Ranges of Variables for Supercritical Cryogenic Hydrogen
Straight Circular Tubes

Reduced Variables		Ratio T_s/T_b	Maximum Heat Flux (cal/cm^2 sec)	Reynolds Number (Maximum)	Tube Orientation
k Fluid perature (T_b)	Surface Temperature (T_s)				
1.25 to 1.44	3.6 to 13.2	2.9 to 10.2	69	31 × 10^5	Horizontal*
0.86 to 3.1	-	-	940	130 × 10^5	Vertical Upward Flow*
0.91 to 1.73	30.5 (Max)	16.5 (Max)	313	17.8 × 10^5	Vertical Upward Flow*
0.93 to 2.5	25.0 (Max)	6.3 (Max)	235	-	Vertical Upward Flow*
0.76	24.0 (Max)	-	92	-	Vertical Upward Flow
0.9 to 5.3	-	-	94	93 × 10^5	No information given
0.66 to 2.0	-	13.0 (Max)	96	-	Vertical Upward Flow
1.6 to 2.3	-	-	34	20 × 10^5	Horizontal*
.0 to 3.3	2.4 to 20.0	11.0 (Max)	290	40 × 10^5	Vertical Upward Flow
.0 to .6	7.2 to 28.0	-	800	-	Vertical Upward Flow

not state the tube orientation explicitly, the information
luced from figures or schematic diagrams

/3. .....

B

3. REVIEW OF EXPERIMENTAL WORK ON FORCED CONVECTION HEAT TRANSFER TO SUPERCRITICAL HYDROGEN

The ranges of experimental data relating to forced convection heat transfer to supercritical hydrogen flowing in straight tubes of circular cross-section have been summarised in Table 1 and are indicated in Fig. 4. Data for curved and non-circular cross section tubes are given in Tables 3 (p.12) and 5 (p.14).

3.1 Straight Circular Tubes

A few supercritical data were obtained by Core et al. (22) in the region of pressure just above the critical ($P_{red.}$ up to 1.13) and with mean bulk fluid temperatures confined to a narrow range close to the critical temperature (30 to 33.5°K). A number of data at the same pressure and mass flow rate in this region show that with increasing heat flux, the local heat transfer coefficient increases to a maximum value and declines with further increase in the heat flux. The range of bulk fluid temperatures is too narrow to draw any conclusions as to the reason for this behaviour.

Thompson and Geery (15) covered wider ranges of pressure and temperature, using para-hydrogen, although reduced pressures below 3.6 were not studied. The authors concluded from their experimental data that heat transfer to supercritical cryogenic hydrogen occurred in two distinct regimes:

Regime "A"

This occurs with bulk fluid temperatures between the critical value and about 80°K, in which heat flux was found to be proportional to 0.7 power of the temperature difference between heated surface and bulk fluid.

The "best-fit" dimensionless correlation for this regime was:

$$Nu = 0.000534\ Re^{1.1}\ Pr^{0.4} \left(\frac{T_s}{T_b}\right)^{-0.64} \quad \text{..... 3}$$

There was wide scatter of experimental data, but the majority were correlated to ± 30% by this expression. This appears to be an unstable region of heat transfer.

Regime "B"

The data for the second regime, representing more stable conditions, with heat flux proportional to the temperature difference, were correlated in similar fashion to give:

$$Nu = 0.0217\ Re^{0.8}\ Pr^{0.4} \left(\frac{T_s}{T_b}\right)^{-0.34} \quad \text{..... 4}$$

It was found that this second equation could also be used to correlate data in Regime "A" with fair accuracy except for those obtained at low heat fluxes and low T_s/T_b ratios.

/The .....

The ranges of parameters for the two regimes are summarised in Table 2.

TABLE 2

Data of Thompson and Geery (15) - Ranges of Parameters

	REGIME "A"	REGIME "B"
Heat Flux, cal/cm^2 sec	4.3 to 192	23.5 to 313
Temperature Difference, surface to fluid, degK	2.8 to 387	117 to 809
Heat Transfer coefficient, cal/cm^2 sec degK	0.08 to 0.81	0.10 to 0.47
Temperature Ratio, T_s/T_b	1.06 to 8.72	3.45 to 16.5
Reynolds Number	2.62 to 13.0 $\times 10^5$	2.96 to 17.5 $\times 10^5$
Prandtl Number	0.73 to 1.70	0.62 to 1.54

From this it can be seen that there is no satisfactory criterion to determine which mode of heat transfer will occur under any given set of conditions. The first expression above agrees quite closely with the equation proposed by Wright and Walters (23) to correlate their data for gaseous normal hydrogen at low heat fluxes; while the relation for Thompson and Geery's Regime "B" is in agreement with the equation of McCarthy and Wolf (24) for heat transfer to gaseous hydrogen at high pressures and heat fluxes.

The authors' claim that their data show the same minimum in the generalised heat transfer coefficient $\left(\frac{h\ D^{0.2}}{G^{0.8}}\right)$ as reported by Powell (13) for cryogenic oxygen at reduced pressure of 1.4 does not seem to be justified. The minima in these experiments with hydrogen, at reduced pressures between 3.6 and 7.2, are associated with the transition from their Regime "A" to Regime "B", rather than with the dependence of fluid properties on temperature near the critical temperature. The phenomenon described is virtually the same at reduced pressures of 3.7 and 7. At these pressures the temperature dependence of fluid properties is relatively slight, even in the vicinity of the critical temperature.

Miller et al. (25,26) give experimental data for turbulent forced convection for cryogenic hydrogen flowing in vertical heated tubes, over a wide range of conditions. Pressures were between 27 and 170 atm, Reynolds numbers (bulk) up to 13×10^6 and the maximum heat flux was 940 cal/cm^2 sec. The data were correlated by the equation of Hess and Kunz (q.v.) which includes a correction for the wall-to-bulk fluid kinematic viscosity ratio.

/At .....

At the lower supercritical pressures studied (reduced pressure of approximately 2), large increases in tube wall temperatures were observed at locations where the bulk fluid temperature was slightly above the critical temperature ("film-boiling" type of effect giving a minimum in the local heat transfer coefficient). This effect was not observed at higher pressures when cryogenic hydrogen behaved in a similar way to hydrogen gas at higher temperatures.

In France, Perroud and co-workers have published a number of papers (27,28,29,30), giving experimental data for forced convection heat transfer to liquid hydrogen in circular tubes, and also in rectangular tubes in which only one side was heated. The number of data in the supercritical region is restricted to the pressure range 13 to 16 atm and for circular tubes only. Fluid (60% para-hydrogen) entered the tubes at 25°K, and surface temperatures up to 800°K were attained. In this region of pressure and surface temperature, sharp increases in wall temperature were commonly encountered at points where the local fluid temperature was in the close vicinity of the critical temperature. Local Nusselt numbers for this region are much below those predicted by the correlations recommended in the above papers for subcritical conditions, in which the physical properties of the fluid are evaluated at the "film" temperature, viz. $T_f = \frac{1}{2}(T_s + T_b)$. Rapid fluctuations in local wall temperature, pressure, and mass flow rate were also observed under these supercritical conditions, but attenuated on further increase in the fluid pressure.

Experimental data on heat transfer to near-critical cryogenic hydrogen are included in the NASA technical note of Hendricks, Graham, Hsu and Friedmann (31), in which they are compared with data obtained for flow of gaseous and two-phase fluid. Vertically positioned circular tubes were used, of between 0.476 cm and 1.287 cm internal diameter, and length 40 to 60 cm. The fluid entered the tubes at temperatures between 22°K and 67°K (only the upward flow direction was investigated) and the range of pressures covered was 5.5 to 55 bars.

A similarity was noted in axial wall temperature distributions for subcritical fluid, and for supercritical conditions where the fluid bulk temperature at the inlet was much below the transposed critical temperature ($T_b << T_m$). In both these cases the wall temperature first rose to a maximum and then declined. There was also a similarity between the observed pressure drops and in the occurrence of fluid oscillations for the two fluid states. Fluid oscillations occurred over limited "unstable" regions of heat flux and fluid flow rate.

The axial position of the peak in surface temperatures occurred, as a crude approximation, where the bulk temperature approached the transposed critical temperature, but also depended sensitively on heat flux, flow rate and the enthalpy of the fluid at the inlet to the heated tube. No functional dependence of surface temperature on these or other parameters could be demonstrated.

Measured heat transfer coefficients were compared with values predicted by the Nusselt film correlation for gaseous hydrogen (as given in Ref. 32), when it was found that the ratio of these two coefficients approached unity as the pressure increased. For example, in a tube of diameter 0.89 cm and at

/axial .....

axial location 11.25 cm from the inlet flange($\frac{l}{D}$ = 12.6) the ratio of experimental to calculated film coefficient was found to have values between 3 and 4 at reduced pressure 1.2 (i.e. 13.8 bars); at 55 bars, or reduced pressure 4.2, the ratio fell to approximately 1.5.

This reference also includes experimental data for the condition of axial heat flux gradient, which was produced by using an electrically heated tube with tapering wall thickness, giving the maximum power generation at the middle of the tube. It was found that the minimum heat transfer coefficient then coincided with the position of maximum heat flux; also that the relative reduction in heat transfer coefficient here was considerably more marked in the case where inlet bulk fluid temperature was low (27.3°K against 37.1°K). In the case of low inlet bulk temperature the initial value of heat transfer coefficient was considerably higher, and in this case the bulk fluid temperature approached the transposed critical value in the high-heat flux region of the tube.

Various methods of correlation are discussed in this note in terms of the Martinelli two-phase parameter, which it had been demonstrated earlier (33) could be reformulated and used to correlate near-critical heat transfer data. The essential features of this method of correlation are discussed in Section 4 below (page 22). In this more recent note the method is considerably modified by inclusion of the Sterman parameter (Sr)* for supercritical fluid* and an entrance effect term; the experimental Nusselt number is based on enthalpy differences.

The new correlation involves considerable computational effort and there is gross scatter of experimental data over the large range of supercritical pressures covered (13.8 - 55 bars). In common with many other proposed supercritical hydrogen heat transfer correlations, the amount of scatter can be reduced to acceptable proportions (in this case within +35 to -25%) if data in the extended entrance section of the tube (L/d < 30) are excluded.

The range of high supercritical pressures (69 - 172.5 bars) was covered in experiments reported in another NASA report by Hendricks, Simoneau and Friedman (34). Liquid hydrogen entered at between 33 and 110°K and flowed upwards through vertical, uniformly heated tubes with diameters between 0.536 and 1.114 cm. Surface temperatures were between 80 and 670°K, and the maximum heat flux was 290 cal/cm^2 sec. Behaviour of the fluid in this range of pressure was completely gas-like, and the majority of the data could be correlated

/using .....

---

*The Sterman number (Sr), originally proposed for use in flow with boiling, through heated tubes, is the ratio of the transverse to axial velocities, and a measure of the penetration of the bulk fluid stream by the vapour generated at the hot wall. In two-phase flow, $\frac{\dot{q}}{\lambda\rho}$ may be regarded as the mean transverse velocity relative to the total wall area.

For supercritical conditions, the Sterman number becomes $\frac{\dot{q}\ \Delta V}{u_b\ \Delta H}$, where

ΔV and ΔH are respectively the enthalpy and specific volume differences between the hypothetical light ("gas-like") and heavy ("liquid-like") species referred to on page 22.

using the Nusselt film type of relation: $Nu_f = C\ Re_f^{\ p}\ Pr_f^{\ 0.34}$, where the exponent p has a value between 0.8 and 0.9, depending on tube diameter.

Oscillations accompanied by a significant increase in heat transfer coefficient were observed under certain restricted conditions with the largest diameter tubes employed (1.114 cm) only. The effect of pressure on this phenomenon is not discussed but oscillations appear to have been confined to the range 69 - 103.5 bars, and there is evidence that they were affected by heat flux. However similar acoustic vibrations were also observed in the apparatus when there was no heating, and this always occurred at very low flow velocities.

3.2 Curvilinear Tubes and Non-circular Cross Sections

The following work includes experimental data obtained with tubes other than straight ones with circular cross-section and are summarised in Table 3.

Hendricks and Simon (35) investigated heat transfer to hydrogen including supercritical pressures (20.7 and 41.4 bars) in curved tubes of various diameters and geometries. The tubes were vertical, and uniformly heated by electric power; the apparatus was a "blow-down" loop. Many of the data were apparently obtained at 10.35 bars (reduced pressure 0.8) and are referred to in discussion as "near-critical": it is with these data that the most pronounced effects of tube curvature are reported. Heat transfer was improved at concave surfaces (viewed from within the tube) and diminished at convex surfaces. The ratio of concave to convex heat transfer coefficients exceeded 3 for data at reduced pressure 0.8, but the magnitude of the ratio depended on the radius of curvature, angular position, tube diameter and fluid structure. The influence of tube diameter makes generalisation of these effects impossible, since heat transfer coefficients at both the convex and concave surfaces may either maximise or minimise depending upon the tube diameter. The ratio h_{conc}/h_{conv} has a minimum value (for 1.77 cm diameter curved tubes) near the point in the tube where fluid bulk temperature equals the transposed critical temperature; for 0.8 cm diameter tubes with 11.1 cm radius of curvature, however, the ratio remained constant.

Contrary to the authors' statement the graphical data for supercritical hydrogen presented indicate that at this pressure (41.4 bars) heat transfer coefficients at both concave and convex surfaces are slightly higher than those predicted by the Dittus-Boelter type of equation for straight tubes. From this graph the ratio h_{conc}/h_{conv} has values between 1 and 1.2 over the length of a 0.95 cm diameter tube with radius of curvature 19 cm.

It seems likely that both the centrifuging and secondary flow effects reported for reduced pressure 0.8 may also occur in curved tubes at pressures immediately above the critical pressure. (It will be noted that supercritical pressures below reduced pressure 1.6 are not covered in the present reference.) However there is some ambiguity in the authors' discussion of their results, because of their omission to make clear the pressure conditions for the data presented and discussed.

/TABLE 3 .....

TABLE 3

Summary of Data for Curvilinear and Non-circular Cross Section Tubes

Authors and Reference	Reduced Pressure	Fluid Temperature, °K	Maximum Surface Temperature, °K	Heat Flux, cal/cm^2 sec	Remarks on Geometry etc.	Tube Orientation
Perroud and Rebiere (29)	0.62	25 to 230	800	72 (Max)	Straight tubes rectangular cross section. Subcritical pressure only	Vertical Upward Flow
Aerojet (See also Table 5) (37)	4.5 to 6.7	36 to 72	910	186 to 375	Curved tubes of circular and non-circular (flattened) cross-section, and various radii of curvature	Vertical Upward Flow
Hendricks and Simon (35)	0.5 0.8 1.6 and 3.2	31 to 60	-	102 (Max)	Circular tubes bent to 4 different radii of curvature	Vertical Upward Flow*

*Not stated explicitly, inferred from schematic diagram given

/Thompson .....

Thompson and Geery (36) carried out an analysis of heat transfer data for liquid hydrogen flowing in both curved and straight tubes. [This report is unobtainable in the UK at present and details are quoted from the later Aerojet report (37) of 1967. It is not clear from this whether any original data are given in Reference 36.] They concluded that the data for pressures 41.4 and 103.5 bars were best represented by the following relation

$$Nu_f = 0.0208\ C_L\ Re_f^{0.8}\ Pr_f^{0.4}\ (1 + 0.01457\frac{\nu_s}{\nu_b}) \quad \ldots \quad 13A$$

This is the expression of Hess and Kunz (38) discussed below (p. 21), with inclusion of C_L, which is a function of bulk fluid temperature, as follows:

TABLE 4

Coolant temp., °K	C_L		Ratio curved/straight
	Straight tube	Curved tube	
27.8	2.0	-	-
31.2	1.73	-	-
33.7	1.48	1.95	1.32
36.1	1.26	1.64	1.30
38.9	1.07	1.37	1.28
41.6	0.93	1.21	1.30
44.5	0.87	1.11	1.28
47.2	0.85	1.10	1.30

(The influence of the radius of curvature on the data is not given in Ref. 37)

Since the enhancement of C_L at low coolant temperatures is apparently not a function of pressure, this influence of fluid temperature cannot be the result of fluid property variations in the region of transposed critical temperature. (In the range of reduced pressure covered, 3.2 to 8.0, these will in any case be relatively slight.) It will be noted that the correlation suggested indicates that the ratio of heat transfer coefficients for curved to straight tubes is constant over the range of bulk fluid temperature quoted.

A second Aerojet REON report, also not available in UK at the time of writing, and dating from May 1963 (39) is also mentioned briefly in Ref. 37. Heat transfer to hydrogen at near critical temperatures and supercritical pressures, and flowing turbulently in straight and curved tubes, was studied in a one-tube geometry. For curved tubes with non-uniform heating some improvement in heat transfer is reported, but it was not possible to generalise the results in a form permitting extrapolation to other design conditions.

/The .....

The 1967 NASA report (37), giving the results of Aerojet studies in support of the Phoebus nozzle development programme, provides the most comprehensive collection of data from US sources on heat transfer to supercritical hydrogen, under conditions of non-uniform heating and for non-circular geometries. The apparatus is a "blow-down" loop, described in Reference 39.

The study includes data for straight tubes of length 7.5 and 15 cm and diameter 0.373 cm, and uniform wall thickness. These tubes were used to determine the effects of coolant temperatures close to the transposed critical temperature on local heat transfer coefficient, and also to demonstrate that high heat fluxes of the order 580 cal/cm^2 sec can be sustained when using supercritical hydrogen as coolant.

The straight tube data are compared with the equation of Hess and Kunz (see p. 21). This underestimates the experimental data, which show considerable scatter, by up to 70% from the correlating equation, but the inclusion of a kinematic viscosity ratio in the relation accommodates widely differing wall temperature regimes. It is attempted to separate the entrance effects from bulk temperature effects in the short tubes. Both trends are in fact slight compared with the amount of scatter of experimental data, although heat transfer coefficients tend to be higher at low bulk temperatures.

The ranges of tube geometry parameters, and of operating conditions for the experiments with curved tubes are summarised in Table 5.

TABLE 5

Summary of Ranges of Test Parameters for Curved-Tubes (Ref. 37)

Parameter	Circular cross-section tubes		Non-circular cross-section tubes	
R_d cm	8.2	4.2	11.3	5.0
R_u cm	16.4	8.2	18.1	8.2
D_e cm	0.44	0.44	0.40	0.40
L/De (heated length)	21 - 68	23 - 47	23 - 69	26 - 51
P bars	59 - 87	61 - 81	75 - 87	60 - 85
T_b °K	36 - 52	40 - 62	44 - 72	39 - 6
T_s °K	108 - 912	145 - 890	226 - 749	93 - 595
G g/cm^2 sec	579 - 894	388 - 748	420 - 477	479 - 825
$\dot{q}$ cal/cm^2 sec	215 - 361	186 - 375	210 - 364	203 - 375

/Figure 1 .....

Figure 5 indicates the form of the tubes and their cross sections. The curved tubes simulated two different nozzle throat geometries, and were used to determine the degree of enhancement of heat transfer coefficients caused by tube curvature. Non-asymmetric heat fluxes were obtained by variation of wall thickness about the periphery of both circular and non-circular tubes (the latter were flattened circular tubes with uniform flow area, as shown in cross section in Figure 5).

The curved tubes had long entrance lengths of over 20 diameters to avoid any entrance or coolant temperature effects. This allowed the establishment of the thermal boundary layers, and preheating of the coolant to a temperature of approximately $45^{\circ}K$ before the fluid reached the curved portion of the tubes. A comparison of the experimental data with the Hess and Kunz relation reveals the following points:

(a) heat transfer coefficients at the concave surfaces (i.e. outside of the curve) were enhanced by factors up to 2:1,

(b) the magnitude of this enhancement decreased when the radius of curvature was increased,

(c) neither asymmetrical heating nor non-circular ducts caused the measured local heat transfer coefficients to be lower than predicted by the Hess and Kunz relation, and

(d) at those positions of the curved tube surfaces corresponding to the highest heat flux encountered in a rocket nozzle, the measured heat transfer coefficients were between 1.0 and 1.4 times the values predicted by the correlating equation of Hess and Kunz.

The significance of the results with curved tubes for the design of the Phoebus-2 nozzle is discussed. Friction factors were investigated and tend to confirm the heat transfer results, though the findings are not conclusive. The occurrence of vibrations was noticed in some tests, but it was not possible to demonstrate any effect on heat transfer.

3.3 Other Geometries

A number of studies have provided data on heat transfer to hydrogen in flow ducts other than electrically heated tubes in test rigs, such as heat exchangers, and these provide additional information on phenomena peculiar to the supercritical state.

A pertinent reference to some observations made under conditions of pool heating is also included in this Section.

Thurston (9) studied the occurrence of pressure oscillations during heat transfer to liquid hydrogen in an apparatus which cooled from ambient to cryogenic temperatures during each run. The nature of the acoustic modes of vibration observed depended very much on the state of the fluid. In the supercritical condition both Helmholtz and open-pipe resonance were noted, also a "supercritical" mode which occurred only when pressures exceeding the critical value were attained. None of these effects was observed when the liquid

/hydrogen .....

hydrogen entered the test section at temperatures above the transposed critical temperature, from which it is concluded that the presence of dense "liquid-like" fluid is a necessary condition for these vibration effects to take place during heat transfer to supercritical hydrogen.

Bartlit and Williamson (40,41), studied transfer of heat between water at near-ambient temperatures and cryogenic hydrogen in simple, one-pass annular heat exchangers. It was found that overall heat transfer coefficients as low as 1/2 to 1/9 of those predicted by the dimensionless correlation of Dittus and Boelter (42) were obtained, unless a swirl-inducing strip was placed in the upstream end of the exchangers, when results in reasonable agreement with the Dittus and Boelter relation were obtained.

These results are explained by a separation between a core of dense hydrogen flowing along the centre of the tube, and the warmer fluid layer at the walls. The effect of pressure is not discussed by the authors, and it is evident from the tabulated data that this phenomenon is not a consequence of supercritical property variations, for all the experiments in which it was observed were conducted at subcritical pressures. The phenomenon described is consistent with the occurrence of film boiling, which would be expected at the large overall values of temperatures difference between the water and the cryogenic fluid, with hydrogen at subcritical pressures. It is not clear whether experiments were also conducted with hydrogen at supercritical pressures and without a swirl inducer in the apparatus; nor whether core-separation effects were observed under these conditions. It was noted, however, that for all runs carried out without a swirl inducer in the exchanger, large pressure oscillations were observed.

Graham et al. (43) studied the effects of acceleration on pool heating of liquid hydrogen at both subcritical and supercritical pressures. From the evidence of the high speed photographs obtained and from the experimental data the authors concluded that the mechanisms of heat transfer in established film boiling and in supercritical heating (respectively) are very similar. At high temperature differences between surface and fluid, the data for supercritical conditions and for film boiling tended to merge into one band; and all supercritical data were characterised by low values of the heat transfer coefficient.

The effect of increased gravity (7 g) on supercritical heating of para-hydrogen was to increase rates of heat transfer by approximately 65%.

4. ANALYSIS OF SUPERCRITICAL HEAT TRANSFER AND CORRELATION OF EXPERIMENTAL DATA

A number of theoretical and semi-theoretical treatments of the problem of convective heat transfer with variable physical properties has been published. In some cases correlating equations have resulted; a number of these are intended for design purposes with liquid hydrogen systems, and experimental data were employed in their derivation.

Deissler's analysis was initially developed (44) to deal with the case of heat transfer to turbulent flow of gases with very high heat fluxes, where the Prandtl number was near unity and constant specific heat, C_p, could be assumed without serious error. The case was further simplified in that viscosity and thermal conductivity could be represented as comparatively simple functions of temperature.

/The .....

The analysis is based on the analogy between transfer of heat and momentum exchange in turbulent flow and employs familiar equations for molecular conduction of heat, and transfer of momentum by shear stress, modified to take account of the additional transfer due to the turbulent motion of eddies in the fluid, viz.

$$\dot{q} = (k + \rho C_p \epsilon_h) \frac{dt}{dy} \qquad \text{..... } \underline{5}$$

$$\tau = (\mu + \rho \epsilon_m) \frac{du}{dy} \qquad \text{..... } \underline{6}$$

It was assumed that the eddy diffusivities for heat and momentum were equal: $\epsilon_h = \epsilon_m$; and further that the expression developed for eddy diffusivity for adiabatic flow conditions can be applied to transfer of heat with variable fluid properties.

Deissler employed two expressions for the eddy diffusivity at a point in the fluid stream; one for locations close to the wall, viz.

$$\epsilon = n^2 uy \left[1 - \exp\left(\frac{-n^2 uy}{\mu/\rho}\right)\right]$$

the second for points at a distance from the wall, viz.

$$\epsilon = m^2 \frac{(du/dy)^3}{(d^2u/dy^2)^2}$$

in which both n and m were assumed to have constant values, derived from experimental data for adiabatic flow of air.

Velocity, temperature and distance from the wall were represented as dimensionless variables, with the dimensionless heat flux as an independent parameter. Velocity and temperature profiles across the fluid stream were calculated by solution of the resulting simultaneous differential equations and these in turn were used to calculate heat transfer coefficients. The method involved tedious calculations, and from a number of such calculations, Deissler and Eian (45) were able to correlate experimental results for air to give Nusselt number as a single function of the Reynolds number, when fluid properties were evaluated at a reference temperature, T_x, where:

$$T_x = T_b + x\,(T_s - T_b) \qquad \text{..... } \underline{7}$$

with $x = 0.4$.

Deissler later developed this analysis to cover the case of heat transfer to turbulent flow of supercritical water (17), which is considerably more complex since $Pr > 1$, and because of the unusual property variations in the critical region, with strong peaks in the specific heat, C_p, and in the

/Prandtl .....

Prandtl number, Pr, close to the critical temperature of the fluid. As previously, profiles of temperature and velocity across the fluid stream were obtained, but because of the nature of fluid property variations with temperature, these profiles had to be calculated separately for each wall temperature initially assumed. The results show a complex dependence of Nusselt number on the dimensionless heat flux parameter, β. In order to eliminate the effect of β it was necessary to determine fluid properties at a reference temperature which was a function of both the wall temperature and the ratio of wall to bulk fluid temperatures

In his discussion of Deissler's paper (17), Eckert shows a simple method of overcoming this difficulty by plotting the reference temperature as a function of the transposed critical temperature, T_m. This effectively reduces the data for different wall temperatures, T_s, to a single curve, from which it is seen that the value of the reference temperature to be used is largely determined by the transposed critical temperature, T_m. It is also noted that in cases when the bulk fluid temperature is close to T_m the correct reference temperature is T_b; similarly that the surface temperature, T_s, should be used as the reference temperature when T_s is close to T_m. Table 6 gives the reference temperature, T_x, to be used for different values of the function of T_b, T_s and T_m.

TABLE 6

$\frac{T_m - T_b}{T_s - T_b}$	T_x
< 0	T_b
0 to 1.0	T_m
> 0	T_s

Goldmann (46) used a similar analytical method to Deissler, but redefined the dimensionless wall-distance and velocity parameters to take account of the assumption that the eddy diffusivity at a point in the flow field is a function of the fluid properties at that point, but is not affected by small variations close to the point. The method allows the calculation of enthalpy and velocity profiles from an assumed set of wall conditions, viz. T_s, $\dot{q}_s$ and τ_s, and correlation of experimental data is in terms of a generalised heat flux parameter:

$$q' = \frac{\dot{q}\, D^{0.2}}{G^{0.8}} = F\,(T_b,\, T_s) \qquad \ldots\ldots \underline{8}$$

/4.1 .....

Hall, Jackson and Khan (47) used Goldmann's basic assumption but extended the analysis to take account of the effect of the greatly increased magnitude of the expansion coefficient:

$$\frac{1}{\rho}\left(\frac{\partial \rho}{\partial t}\right)_P = f(t)$$

of the fluid close to the heated wall when this is close to the transposed critical temperature. They supposed that this must enhance the turbulent diffusivity in the wall region in proportion to the degree of thermal expansion in the fluid, which sharply maximises at the transposed critical temperature. The modified theory shows reasonable agreement with the trends of their experimental data which were obtained with turbulent flow of supercritical carbon dioxide between parallel plates, under conditions of fully developed velocity and temperature profiles across the flow. The model proposed here is in essence the "boiling-like" mechanism of Goldmann (5), but use of the maxima in thermal expansion coefficient allows this effect to be expressed quantitatively. It is interesting to note that agreement between experiment and theory above is improved by introducing a scaling-factor to the turbulent diffusivity distribution in the sub-layer region (both distributions are consistent with accepted velocity distribution data for the region). The scaling-factor used by Hall et al. fell linearly from a value of 20 at the wall to unity near the edge of the sub-layer, and thus represents a considerable distortion of the original distribution. Figure 6 indicates a hypothetical distribution of eddy diffusivity:

$$\epsilon_a = \bar{y}\left[1 - \exp(-\bar{y})\right]$$

where ϵ_a is in arbitrary units, and $\bar{y} = \frac{y}{y^*}$ is the dimensionless wall distance, y^* being the thickness of the laminar sub-layer. The figure also shows this distribution multiplied by the scaling-factor employed by Hall et al. In reality the diffusivity will also depend on velocity gradient and properties of the fluid (notably the kinematic viscosity) as functions of the wall distance $\bar{y}$.

Nevertheless, it is seen that the modification in distribution B of Fig. 6 represents a significant increase in the influence of turbulence eddies within the sub-layer, which is required to enable the thermal expansion mechanism proposed to fully account for the increases in heat transfer coefficients observed experimentally. Under conditions remote from the critical state it is evidently possible to use a number of different distributions of eddy diffusivity within the sub-layer which will be consistent with measured velocity distributions, and will also enable fair agreement with heat transfer experiments to be obtained. When near-critical conditions exist at the wall it is suggested that the analysis is far more sensitive to the ϵ distribution assumed, since this is in effect "amplified" by the nature of fluid property variations within the layer.

/The .....

The experiments of Hall et al. (47) did not of course involve conditions under which deterioration of local heat transfer is observed, such as has been described for certain conditions in normal pipe flow. Neither does their theory outlined above predict such behaviour which has been discussed earlier in terms of the influence of buoyancy forces (p. 4).

Evidence of periodic heat transfer fluctuations in the laminar sub-layer is given in a recent experimental study by Armistead and Keyes (48) of turbulent flow of unpressurised water, using hot film sensors. This demonstrates the existence of moderately high levels of turbulence in the laminar sub-layer, and gives further cause to speculate whether the eddy diffusivity distributions employed in many theoretical models for supercritical heat transfer omit some important turbulence promoting mechanism occurring in the laminar region.

Hsu and Smith (49), modified Deissler's treatment of the problem to take account of the effect of the variation of fluid density across the stream on the local values of the eddy diffusivities:

$$\tau = \epsilon_m^* \left[\frac{d}{dy}(\rho u)\right] \qquad \text{..... } \underline{9}$$

where $$\epsilon_m^* = \epsilon_m \left[1 + u\frac{d\rho}{dy} \Big/ \rho\frac{du}{dy}\right]$$

The procedure for calculating velocity and temperature profiles, and hence heat transfer coefficients and Nusselt numbers, was similar to that in the analyses already discussed.

For flow in vertical tubes, the influence of large fluid density variations in inducing natural convection in near-critical heat transfer was considered. The analysis predicts that Nusselt numbers should be increased under conditions where the transposed critical temperature lies between the wall and bulk fluid temperatures. The effect should only be significant for low Reynolds numbers and relatively high Grashof numbers, since the gravitation forces are increased in proportion to the ratio Gr/Re^3.

Szetela (50) obtained experimental data for hydrogen at bulk temperatures between 33.3 and 47°K, wall to bulk temperature ratios from 3 to 11 and reduced pressures of 1.13 and 1.68. A limited number of data were selected and calculations made to obtain predicted values of the heat transfer coefficients from the equations of Deissler (17) and Hsu and Smith (49), at the same conditions. Heat transfer coefficients calculated from the unmodified equations of Deissler all fall <u>below</u> the experimental values by differences ranging up to 33%. The coefficients calculated from Hsu's modified equations were from 50 to 75% <u>above</u> the experimentally measured data.

These analyses have therefore proved inadequate to deal with the extreme variation of fluid properties with temperature in the critical region for hydrogen; also, experiments indicated large variations in temperature along the tube wall, whereas the theoretical treatments discussed above assume uniform wall temperature. It also proved impossible to correlate the data using the conventional dimensionless relation for Nusselt number, with fluid properties evaluated at the "film" temperature, T_f, because of excessive scatter of the data.

/A semi-empirical ...

A semi-empirical study was made by Hess and Kunz (38), and the results compared with data from the literature for hydrogen in the supercritical region. This analysis starts from the same basic equations as those previously discussed, but employs a single expression for the momentum eddy diffusivity:

$$\epsilon_m = K^2 y^2 [1 - \exp(\frac{-y}{A})]^2 \frac{du}{dy} \quad \ldots\ldots \underline{10}$$

the factor in brackets accounting for viscous damping of turbulent eddies in the region close to the wall. A comparison was made of the computed Nusselt numbers with experimental values derived from References 33 and 50 and additional unpublished data. At low heat fluxes good agreement was obtained, but with increasing heat flux, the ratio Nu (expt)/Nu (calc) increased markedly. It was found that the increase in this ratio could be correlated as a linear function of the kinematic viscosity ratio, ν_s/ν_b $[\nu = \mu/\rho]$. The maximum value of this ratio in the experimental data considered was 140, and it is evident that the analysis was unable to account for the variation in fluid properties across the stream under such extreme conditions.

Since the largest variations in fluid properties occur close to the wall, the value of the "damping factor" A^+ in the non-dimensional form of the expression for eddy diffusivity, viz:

$$\frac{\epsilon_m}{(\mu/\rho)} = K^2 (y^+)^2 [1 - \exp(\frac{-y^+}{A^+})]^2 \frac{du^+}{dy^+} \quad \ldots\ldots \underline{11}$$

was examined more closely. Values of A^+ were calculated to give agreement between the experimental and computed values of Nusselt number for data obtained over a wide range of heat flux, and it was found possible to correlate these values with the kinematic viscosity ratio:

$$A^+ = 30.2 \exp(0.0285 \frac{\nu_s}{\nu_b}) \quad \ldots\ldots \underline{12}$$

After substituting this expression for A^+ in the original expression for eddy diffusivity, it was found that the resulting equation gave good agreement with the experimental data for l/D values greater than 30, but very poor agreement with l/D < 30. The latter case also corresponded to the condition where $T_b < T_m$ and it is argued by Hendricks and Hsu in their discussion of the original paper that this poor agreement can be explained on the basis of the behaviour of the viscosity ratio, ν_s/ν_b, and hence of the damping factor A^+ as T_b approaches T_m. Hess and Kunz, however, explain the lack of agreement as the result of an extended entrance region in the heated tube. As with the other theoretically derived relations for heat transfer to turbulent flow of supercritical fluids, the method involves complex and time consuming calculations. The authors therefore propose a modification of the conventional equation: $Nu_f = F(Re_f, Pr_f)$ for design purposes, in which the deviation between experimental and computed Nu values is represented as a function of the kinematic viscosity ratio:

/Equation .....

$$Nu_f = 0.0208 \left[\frac{\rho_f u_b D}{\mu_f} \right]^{0.8} Pr_f^{0.4} \left[1 + 0.01457 \left(\frac{\nu_s}{\nu_b}\right)\right] \qquad \text{..... 13}$$

The majority of the data were correlated by this relation to ± 20%.

An earlier attempt to correlate data for heat transfer to turbulently flowing supercritical hydrogen was made by Hendricks et al. (33) and relies upon a suggested similarity between forced convection film boiling and heat transfer to fluid at near-critical conditions. Experimental data are presented for both these regions of convective heat transfer to hydrogen (33,51).

The scheme for correlation of supercritical data uses a pseudo two-phase model for the near-critical fluid state. It is postulated that the supercritical region is an extension of the two-phase region, and that fluid in the near-critical state consists of an aggregate of two types of molecule clusters. The fluid is taken, for simplicity, to consist of: (a) a heavy species corresponding to the tightly packed liquid structure, with its density (ρ_{melt}) equal to that of liquid hydrogen at the melting temperature, and (b) a light species, with density ρ_g corresponding to that of a perfect gas at the bulk fluid temperature, viz.

$$\rho_{g,b} = \frac{PM}{RT_b} \qquad \text{..... 14}$$

The mass and volume fractions of the respective species can then be readily obtained for supercritical hydrogen in any condition, from a knowledge of the density, as a function of the temperature and pressure. The bulk density is given by

$$\frac{1}{\rho_b} = \frac{x_2}{\rho_{g,b}} + \frac{1 - x_2}{\rho_{melt}} \qquad \text{...... 15}$$

where x_2 is the mass fraction of the gaseous species.

The mechanism for the boiling-like process envisaged was described as follows: "Instead of two phases, there would be a continuum of densities between a light gas-like species and a heavy liquid-like species. Heavy, tightly-packed clusters of molecules would migrate toward the wall and then would be broken up into smaller and lighter clusters and migrate toward the core of the fluid".

Hendricks et al. had been able to correlate their data for film boiling of liquid hydrogen (51) by means of two parameters: the Martinelli factor, X_{tt}, and a predicted Nusselt number, Nu', defined by

$$X_{tt} = \left(\frac{1 - x_2}{x_2}\right)^{0.9} \left(\frac{\mu_{melt}}{\mu_f}\right)^{0.1} \left(\frac{\rho_f}{\rho_{melt}}\right)^{0.5} \qquad \text{..... 16}$$

$$Nu' = 0.023 \left[\frac{\rho_f u_{av} D}{\mu_f}\right]^{0.8} Pr_f^{0.4} \qquad \text{..... 17}$$

/In .....

In Equation 17 the fluid density, ρ_f, at the film temperature, T_f, was defined by

$$\frac{1}{\rho_f} = \left(\frac{x_2}{\rho_{g,f}}\right) + \left(\frac{1 - x_2}{\rho_{melt}}\right) \qquad \text{..... } \underline{18}$$

where x_2 is the mass fraction of the gaseous species.

By plotting the ratio Nu(expt.)/Nu' as ordinate against the Martinelli parameter for the supercritical data, a very similar result to that obtained with the data for film boiling was obtained.

The correlating equation is of the form:

$$\text{Nu(expt.)} = \frac{\text{Nu}'}{(0.611 + 1.93\, X_{tt})} \qquad \text{..... } \underline{19}$$

The method yields satisfactory correlation of the experimental data over wide ranges of heat flux and mass flow rate, although the procedure for calculating heat transfer coefficients is somewhat complicated. The ratio of experimental Nusselt numbers to those predicted by the conventional "pipe flow" equations may have values of up to 3 in the near-critical region, giving support to the concept of an additional (boiling-like) mechanism enhancing turbulent transfer of heat to the fluid. Use of the pipe flow equations in design, while these are extremely conservative, could lead to difficulty in the near-critical region in that the additional heat gained by the fluid from the wall would result in large density changes and increase in fluid velocity in the coolant passages, ("vapour choking") and incorrect estimation of the state of the fuel at the point of injection prior to combustion. However, the conventional pipe flow equation, with fluid properties measured at "film" temperature:

$$\text{Nu}_f = 0.023\, \text{Re}_f^{0.8}\, \text{Pr}_f^{0.4} \qquad \text{..... } \underline{20}$$

will correlate data for near-gaseous supercritical hydrogen to ± 15%, over wide ranges of temperature and pressure, provided that the fluid exhibits no unusual or rapid changes in properties with temperature.

An important restriction on the pseudo-two-phase correlation is that the bulk fluid temperature must be near or above the transposed critical temperature, T_m. In practice this will not limit the usefulness of the correlation seriously, since the critical temperature for hydrogen is only a little above the normal boiling temperature (33°K and 20°K respectively) and for those pressures where the supercritical effects are likely to be serious, the transposed critical temperature will be only slightly higher than the critical temperature.

A number of correlating equations which have been proposed for heat transfer to supercritical hydrogen have been referred to above. Williamson and Bartlit (52) compared seven different correlations which have been proposed for hydrogen, and also the simple "pipe flow" equation of Dittus and Boelter, with experimental

/data .....

data for hydrogen from all known sources, covering a range of fluid temperatures from 33 to 280°K, and pressures from 1.7 to 97 bars. They found that although individual correlating equations usually fitted best the data for which they were proposed, the best correlation for data from all the sources was the Dittus and Boelter equation, but with the initial constant term halved, viz.

$$Nu_b = 0.012\, Re_b^{0.8}\, Pr_b^{0.4} \qquad \ldots\ldots\ 21$$

This correlated 70% of all the experimental data at film temperatures between 55 and 280°K, to ± 20%, although scatter in the vicinity of the critical temperature (T_c = 33°K) was much greater, as would be expected.

For prediction of heat transfer coefficients at near-critical conditions, where fluid bulk temperatures are below 50°K, it is recommended that approximate values should be estimated from available experimental data in this region; or from correlations such as Equation 13, due to Hess and Kunz, for which some reliability has been demonstrated by experiment (38) at supercritical conditions.

The Hess and Kunz correlation appears to give conservative predictions of heat transfer in curved tubes also, and is recommended as a design equation for these geometries when modified to account for the enhancement of mean heat transfer coefficients produced by tube curvature.

5. SPECIAL EFFECTS WITH HEAT TRANSFER TO LIQUID HYDROGEN: PARA- TO ORTHO-CONVERSION

The possibility exists that heat transfer to cryogenic hydrogen may be influenced by the conversion of the para- to the ortho- form of hydrogen, since the equilibrium composition of liquid hydrogen varies with temperature as follows:

Temperature, °K	% Para-H_2	% Ortho-H_2
20	99.8	0.2
77	50	50
300	25	75

Liquid hydrogen used in operational rocket engines (and in the majority of the experimental studies reported), is usually catalytically converted to give a very high proportion of para-hydrogen prior to liquefication. This prevents subsequent high evaporation losses due to the gradual conversion of the ortho- to the para- form, with evolution of heat comparable to the latent heat of evaporation of hydrogen.

When liquid para-hydrogen at cryogenic temperatures comes into contact with surfaces at temperatures several hundred degrees Kelvin higher, rapid conversion of para- to ortho- could take place, this representing an additional

/heat .....

heat sink. The most probable mechanism for this conversion is a reaction at the hot wall, possibly catalysed by the material of the surface, e.g. stainless steel or nickel alloy.

Hendricks et al. (51) attempted to calculate the contribution of the para- to ortho- conversion to the forced convection heat transfer to sub-critical cryogenic hydrogen, assuming that the reaction was first order, requiring the diffusion of the ortho- and para- species through the laminar boundary layer at the wall. They concluded that the conversion could have made no perceptable difference to the amount of heat transferred to the fluid. Experimental results with para-hydrogen in which both stainless steel and gold-plated heated surfaces were employed, tended to confirm this finding.

Thompson and Geery (15), used 100% para-hydrogen at supercritical pressures (P_{red} 3.6 to 7.1) and noted from study of the heat balances in the experiments that the ratio $\frac{\text{electrical power input}}{\text{change in fluid enthalpy}}$ increased with wall temperature.

They concluded that an appreciable fraction of para-hydrogen was converted to ortho-hydrogen at high wall temperatures, with absorption of the endothermic heat of reaction. The degree of conversion was apparently a function of both the wall temperature and the residence time of the fluid in the heated tube; the latter was only of the order 30 milliseconds. It is conceivable that heat losses from the apparatus may account for these observations.

Perroud and Rebière (28) compared heat transfer to 95% para-hydrogen and to 60% para-hydrogen under identical experimental conditions and found no difference which could be attributed to the para- to ortho- conversion.

No studies are known in which the ortho-/para- composition of the fluid at the inlet and outlet from the heated section was measured simultaneously during the experiments.

6. CONCLUSIONS

It is evident from this survey that no consensus is obtained from the published data regarding the nature of heat transfer to hydrogen under near critical conditions. A number of investigations strongly suggest that under these conditions the fluid behaves as if two "pseudo-phases" exist during turbulent flow through heated tubes, with some similarities to the behaviour of boiling liquids. Additional evidence is available to support this concept from the data for other fluids in the same region of reduced pressure and temperature. A convincing model for the mechanism of pseudo-two phase heat transfer is not so far available.

The theoretical and semi-theoretical analyses considered attempt to take account of the severe variations with temperature of fluid properties, and discount the possibility of additional heat transfer from pseudo-two phase behaviour. Such analyses are of limited practical usefulness because of their complexity in application, and have proved less successful in predicting heat transfer to near-critical hydrogen than to carbon dioxide and water in this thermodynamic region. The lack of completely reliable data for a number of the thermal and transport properties of hydrogen in the critical region may partly account for this.

/Under .....

Under most conditions of heat transfer to cryogenic hydrogen at super-critical pressures, the correlation of Hess and Kunz gives conservative estimates of convective heat transfer coefficients. In general mean coefficients in curved tubes appear to be up to 30% higher than for the same conditions in straight tubes. However, local heat transfer coefficients at the concave and convex walls of curved tubes may be widely different, with diminished heat transfer at the inside of the curve. But it is impossible to generalise these effects from the available experimental data because of the influence of tube diameter and other parameters.

In the case of asymmetrical axial heat flux distribution, a severe minimum in the local heat transfer may occur at the position of maximum heat flux, and this effect is exacerbated where the fluid temperature at this critical location is close to the transposed critical temperature of the fluid.

The available experimental data suggest that neither non-circular tube cross-sections, nor asymmetry of the peripheral heat flux distribution produce adverse effects on heat transfer to supercritical hydrogen when employed as a coolant.

There are no experimental data published for heat transfer to hydrogen in multi-tube assemblies. With an arrangement of several tubes in parallel between common manifolds flow instabilities could result for cryogenic hydrogen at supercritical pressures, in the case of non-uniform distribution between the tubes. This has obvious application to the cooling problem in a hydrogen-fuelled rocket engine, and one would anticipate that the condition would become more severe as the fluid pressure approached the critical pressure.

/7. .....

7. REFERENCES

1. Dean, L.E. and Petrozzi, P.J., "Heat transfer conditions occurring in a hydrogen cooled combustion chamber", ARS Paper No. 1712-61 (1961)

2. Sieder, E.N. and Tate, G.E., Ind. Engng. Chem. ind. Edn., 28, 1429 (1936)

3. Sengers, J.V. and Mechels, A., "Progress in International Research on Thermodynamic and Transport Properties, Princeton University, Jan. 1962", (eds. J.F. Masi and D.H. Tsai), Academic Press, p. 434

4. Ziebland, H. and Needham, D.P., ibid, p. 441

5. Goldmann, K., Paper No. NDA-2-31, Reactor Heat Transfer Conference, New York City, Nov. 1956

6. Swenson, H.S. et al., J. Heat Transfer, 87C, 477 (1965)

7. Dickenson, N.L. and Welch, C.P., ASME Trans., 80, 746 (1958)

8. Griffith, J.D. and Sabersky, R.H., ARS J., 30, (3), 289 (1960)

9. Thurston, R.S., Proc. 1964 Cryogenic Engineering Conference, Advances in Cryogenic Engineering, Plenium Press, N.Y., Vol. 10A, Paper I-2, p. 305 (1965)

10. Hines, W.S. and Wolf, H., ARS J., 32, 361 (1962)

11. Cornelius, A.J. and Parker, J.D., Proc. 1965 Heat Transfer and Fluid Mechanics Inst., Stanford Univ. Press

12. Koppel, L.B. and Smith, J.M., Papers Presented at the 1961 Int. Heat Transfer Conference Aug - Sep, ASME, Paper No. 69, 585 (1961)

13. Powell, W.B., ARS J., 27, (7), 776 (1957)

14. Shitsman, M.E., High Temperature, 1, (2), 237 (1963)

15. Thompson, W.R. and Geery, E.L., Adv. cryogen. Engng. 7, Paper J-5, 391 (1962)

16. Wood, R.D. and Smith, J.M., AIChE J., 10, (2), 180 (1964)

17. Deissler, R.G., ASME Trans., 76, 73 (1954)

18. Shitsman, M.E., "Natural convection effects on heat transfer to a turbulent water flow in intensively heated tubes at supercritical pressures"; Symposium on Heat Transfer and Fluid Dynamics of Near-Critical Fluids, Bristol, Instn. mech. Engrs. (London) (March 1968)

/19. .....

19. Miropolskiy, Z.L. et al., "Regimes of deteriorated heat transfer at forced flow of fluids in curvilinear channels", Third Int. Heat Transfer Conference, Chicago, AIChE (August 1966)

20. Brown, C.K. and Gauvin, W.H., Can. J. chem. Engng, 43, 306 (1965)

21. Brown, C.K. and Gauvin, W.H., Chem. Engng Sci., 21 (11), 961 (1966)

22. Core, T.C. et al., "Heat Transfer Studies", Report No. WADD-60-239 (Sept. 1959)

23. Wright, C.C. and Walters, H.H., "Single tube heat transfer tests - gaseous and liquid hydrogen", WADC TR 59-423 (August 1959)

24. McCarthy, J.R. and Wolf, H., ARS J., 30, 423 (1960)

25. Miller, W.S. et al., "Forced convection heat transfer to liquid hydrogen at supercritical pressures". Paper presented at the International Institute of Refrigeration Conference, Grenoble, June 1965

26. Miller, W.S. et al., Rocketdyne Report No. R-6129 (1965)

27. Perroud, P. and Rebiere, J., Centre d'Etudes Nucleaires de Grenoble, Report No. CEA-R2439 (1964)

28. Perroud, P. and Rebiere, J., Centre d'Etudes Nucleaires de Grenoble, Report No. CEA-R2499 (1964)

29. Perroud, P. and Rebiere, J., Centre d'Etudes Nucleaires de Grenoble, Report No. CEA-R2796 (1965)

30. Perroud, P. et al., "Convection force'e de l'azote et de l'hydrogene liquides", Centre d'E.N.d.G. Note CENG./ASP. No. 65-07. Paper given at the Int. Inst. Refrig. Conference, June 1965

31. Hendricks, R.C. et al., NASA TN D-3095 (1966)

32. Taylor, M. and Kirchgessner, T.A., NASA TN D-133 (1959)

33. Hendricks, R.C. et al., ARS J., 32, (2), 244 (1962)

34. Hendricks, R.C., Simoneau, R.J. and Friedman, R., NASA TN D-2977 (Sept. 1965)

35. Hendricks, R.C. and Simon, F.F., Proc., Multi-phase Flow Symposium, (H.J. Lipstein ed.) ASME, 90 (1963)

36. Thompson, W.R. and Geery, E.L., Aerojet REON Report RN-S-0274 (April 1966)

37. Anon., Aerojet Report, NASA CR-678 (Feb. 1967)

38. Hess, H.L. and Kunz, H.R., J. Heat Transfer, 87, (1), 41 (1965)

/39. .....

39. Anon., Aerojet REON Report 2551 (May 1963)

40. Bartlit, J.R. and Williamson, K.D., Paper H-6, Proc. 1965 Cryogenic Engineering Conference, Houston, Texas

41. Williamson, K.D. and Bartlit, J.R., Proc. 1964 Cryogenic Engineering Conference, Advances in Cryogenic Engineering, Vol. 10A (1965)

42. Dittus, F.W. and Boelter, L.M.K., Univ. Calif., Publs Engng, 2, 443 (1930)

43. Graham, R.W. et al., Int. Adv. Cryogen. Engng, 10B, Paper T-2, 342 (1965)

44. Deissler, R.G., NACA TN 2242 (1950)

45. Deissler, R.G., and Eian, C.S., NACA TN 2629 (1952)

46. Goldmann, K., "Nuclear Engineering", Chem. Engng Progress Symposium Series, 50, (11) (1954)

47. Hall, W.B., Jackson, J.D. and Khan, S.A., Proc. 3rd Intern. Heat Transfer Conf. Chicago, Illinois, AIChE, 257 (1966)

48. Armistead, R.A. and Keyes, J.J., J. Heat Transfer, 90C, (1), 13 (1968)

49. Hsu, Y.Y. and Smith, J.M., ASME Paper No. 60-HT-8 (April 1960)

50. Szetela, E.J., ARS J., 32, 1289 (1962)

51. Hendricks, R.C. et al., NASA TN D-765 (1961)

52. Williamson, K.D. and Bartlit, J.R., "Forced convection heat transfer to flowing hydrogen, 60-500°R", Los Alamos Scientific Laboratory, University of California (1965)

/NOMENCLATURE .....

NOMENCLATURE

A	damping factor for growth of turbulent eddies (Eqn. 10 and Ref. 38)	(cm)
A^+	non-dimensional damping factor	
C_p	specific heat at constant pressure	(cal/g degK)
D	tube diameter	(cm)
D_e	effective diameter for non-circular channel geometry	(cm)
g	gravitational acceleration	(cm/sec^2)
G	mass flow rate	(g/cm^2 sec)
h	heat transfer coefficient	(cal/cm^2 sec degK)
H	enthalpy of fluid	(cal/g)
k	thermal conductivity	(cal/cm sec degK)
K	turbulence mixing length (Eqn. 10)	(cm)
l	length along heated surface	(cm)
m n	constants in the expressions for eddy diffusivity (Ref. 17)	
M	molecular weight	
P	pressure	(atm)
P_c	critical pressure	(atm)
P_{red}	reduced pressure ($P_{red} = P/P_c$)	
$\dot{q}$	heat flux	(cal/cm^2 sec)
q'	generalised heat flux $\left(q' = \dot{q}\,\frac{D^{0.2}}{G^{0.8}}\right)$	
R_u, R_d	upstream and downstream radii of curvature in curved tubes	(cm)
R	gas constant	(cal/degK mole)
T	temperature	($^\circ$K)
T_{red}	reduced temperature	

$/T_c$ .....

T_c	critical temperature	(°K)
T_f	film temperature $[T_f = \frac{1}{2}(T_b + T_s)]$	(°K)
T_m	transposed critical temperature (i.e. the temperature at which the specific heat C_p attains its maximum value at a given supercritical pressure)	(°K)
T_x	reference temperature $[T_x = T_b + x(T_s - T_b)]$ for evaluation of fluid properties in variable-property heat transfer analysis (Ref. 17)	(°K)
u	velocity in stream parallel to heated surface	(cm/sec)
v	specific volume	(cm^3/g)
x_1	fraction of heavy "liquid" species in near-critical fluid (Ref. 33)	
x_2	fraction of light "gaseous" species (Ref. 33)	
y	distance from heated surface	(cm)
y^+	dimensionless wall distance $[y^+ = \frac{y(\tau_s/\rho_s)^{\frac{1}{2}}}{(\mu_s/\rho_s)}]$	
β	heat flux parameter $\beta = \left[\frac{\dot{q}_s\,(\tau_s/\rho_s)^{\frac{1}{2}}}{Cp_s g \tau_s T_s}\right]$	(p. 18 Ref. 17)
ϵ_h	eddy diffusivity (thermal)	(cm^2/sec)
ϵ_m	eddy diffusivity (momentum)	(cm^2/sec)
ϵ_m^*	momentum eddy diffusivity corrected for variation of fluid density across stream	(cm^2/sec)
λ	latent heat of vaporisation	(cal/g)
μ	dynamic viscosity	(g/cm sec)
ρ	density	(g/cm^3)
ρ_g	density of perfect gas (Ref. 33 and Eqn. <u>14</u>)	(g/cm^3)
ρ_{melt}	density of liquid at the melting point	(g/cm^3)
ρ_f	film density for pseudo-two phase fluid (Eqn. <u>18</u>)	(g/cm^3)
τ	shear stress	($g/cm\ sec^2$)
ν	kinematic viscosity ($\nu = \mu/p$)	(cm^2/sec)

/<u>Dimensionless</u> .....

Dimensionless Groups

Gr Grasshof number $\left(Gr = \left(\frac{(\rho_b - \rho_s)\ g\rho D^3}{\mu^2}\right)\right)$

Nu Nusselt number $(Nu = hD/k)$

Pr Prandtl number $(Pr = \mu Cp/k)$

Re Reynolds number $(Re = GD/\mu)$

Sr Sterman number $\left(Sr = \frac{\dot{q}}{\lambda\rho u_b}\right)$

Subscripts

av average

b condition or property in the bulk fluid stream

f film condition

g gas

s at heated surface

m at transposed critical temperature

S. No. 60/69/CJ

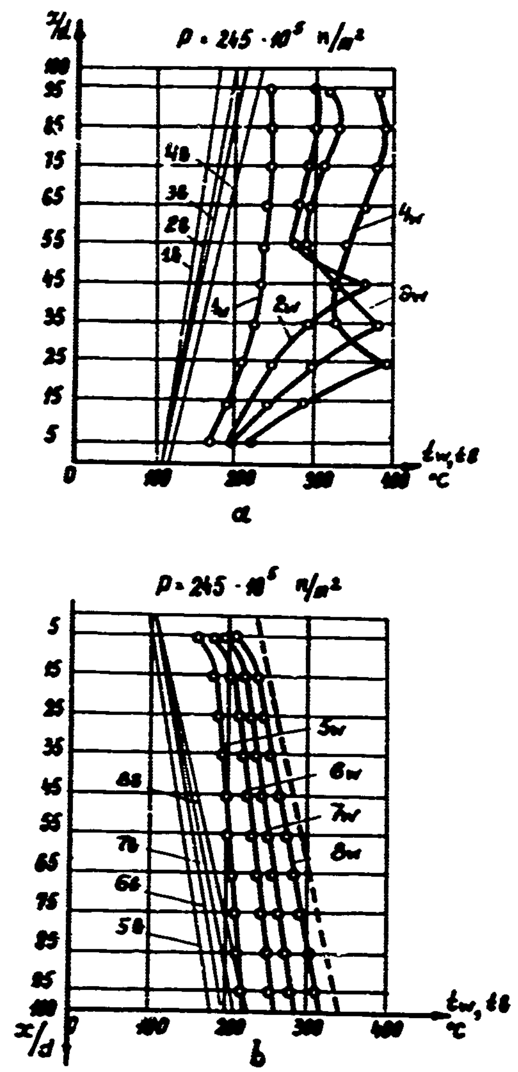

a Upward water flow. *b* Downward water flow.

$P = 245 \times 10^5$ N/m²

1. $G = 382$ kg/m² s, $q = 0{\cdot}27$ MW/m²
2. $G = 382$ „ , $q = 0{\cdot}37$ „
3. $G = 400$ „ , $q = 0{\cdot}45$ „
4. $G = 375$ „ , $q = 0{\cdot}52$ „
5. $G = 400$ „ , $q = 0{\cdot}27$ „
6. $G = 400$ „ , $q = 0{\cdot}36$ „
7. $G = 393$ „ , $q = 0{\cdot}43$ „
8. $G = 281$ „ , $q = 0{\cdot}5$ „

Bulk (b) and wall (w) temperature distribution along the tube

FIG.1. EFFECT OF DIRECTION OF FLOW IN HEAT TRANSFER TO NEAR-CRITICAL WATER IN VERTICAL TUBES, FROM SHITSMAN (18)

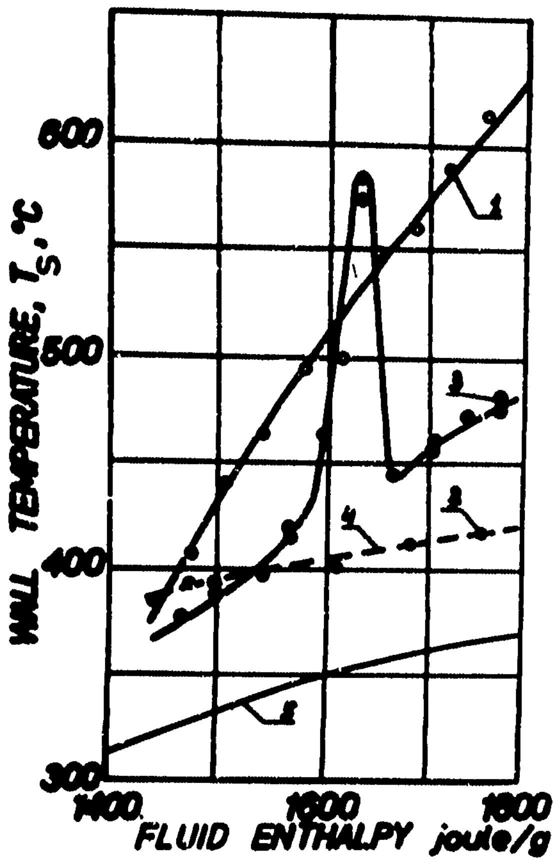

EXPERIMENTAL CONDITIONS

P = 245 bars
G = 60 g/cm² sec
$\dot{q}$ = 12·4 cal/cm² sec
D = 1·6 cm

1 - HORIZONTAL PIPE, THE TOP OF THE WALL ;
2 - HORIZONTAL PIPE, THE BOTTOM OF THE WALL ;
3 - VERTICAL PIPE, UPWARD FLOW ;
4 - FROM $Nu = C\, Re_f^{0.8} Pr_{min}$
5 - FLUID TEMPERATURE.

FIG.2. WALL TEMPERATURES OF THE STRAIGHT PIPES AT SUPERCRITICAL PRESSURES vs. FLUID ENTHALPY, FROM MIROPOLSKIY ET AL. (19)

FIG. 3. NEAR – CRITICAL HEAT TRANSFER TO FLOWING KEROSINE

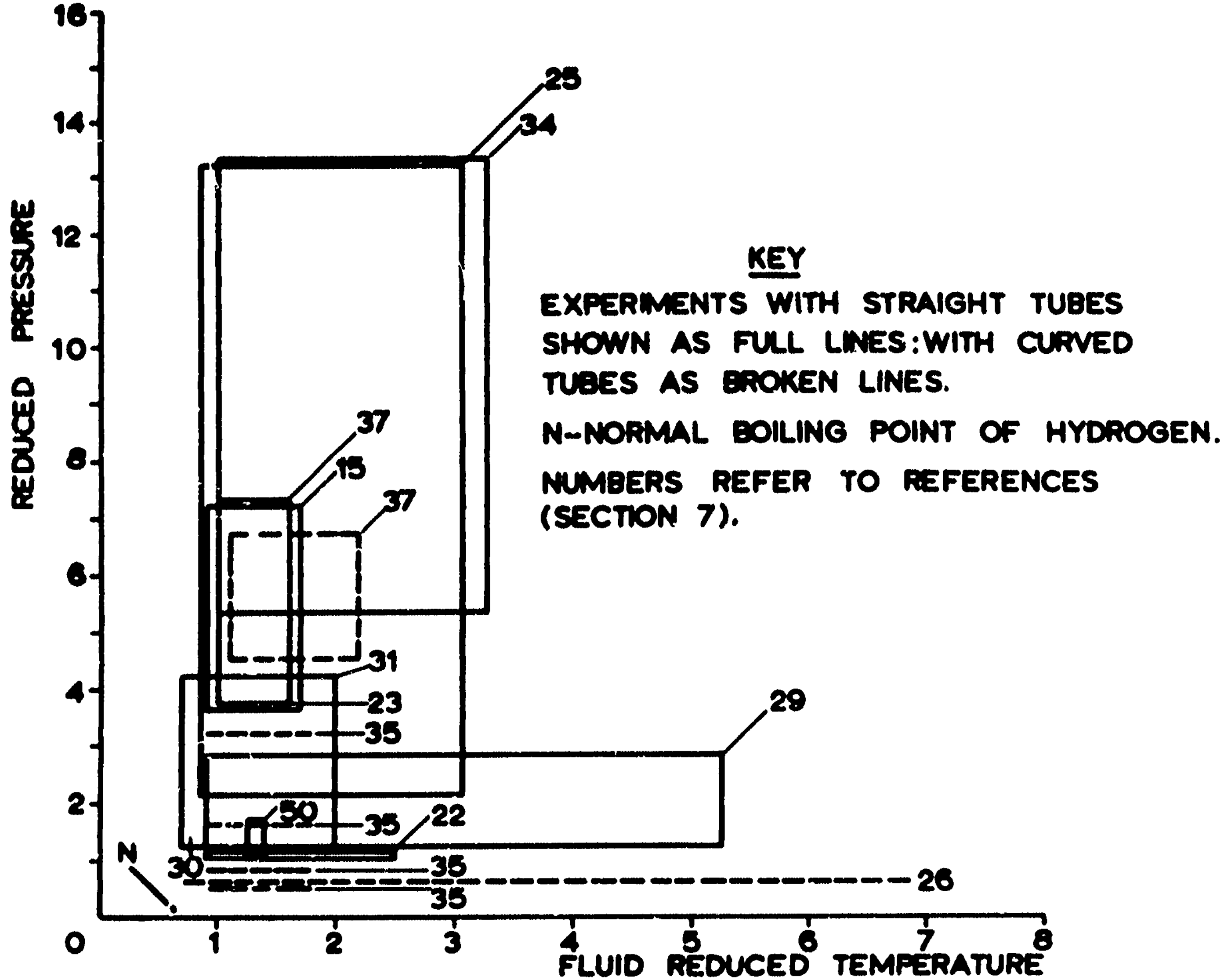

FIG. 4. RANGES OF TEMPERATURE AND PRESSURE IN PUBLISHED EXPERIMENTAL WORK.

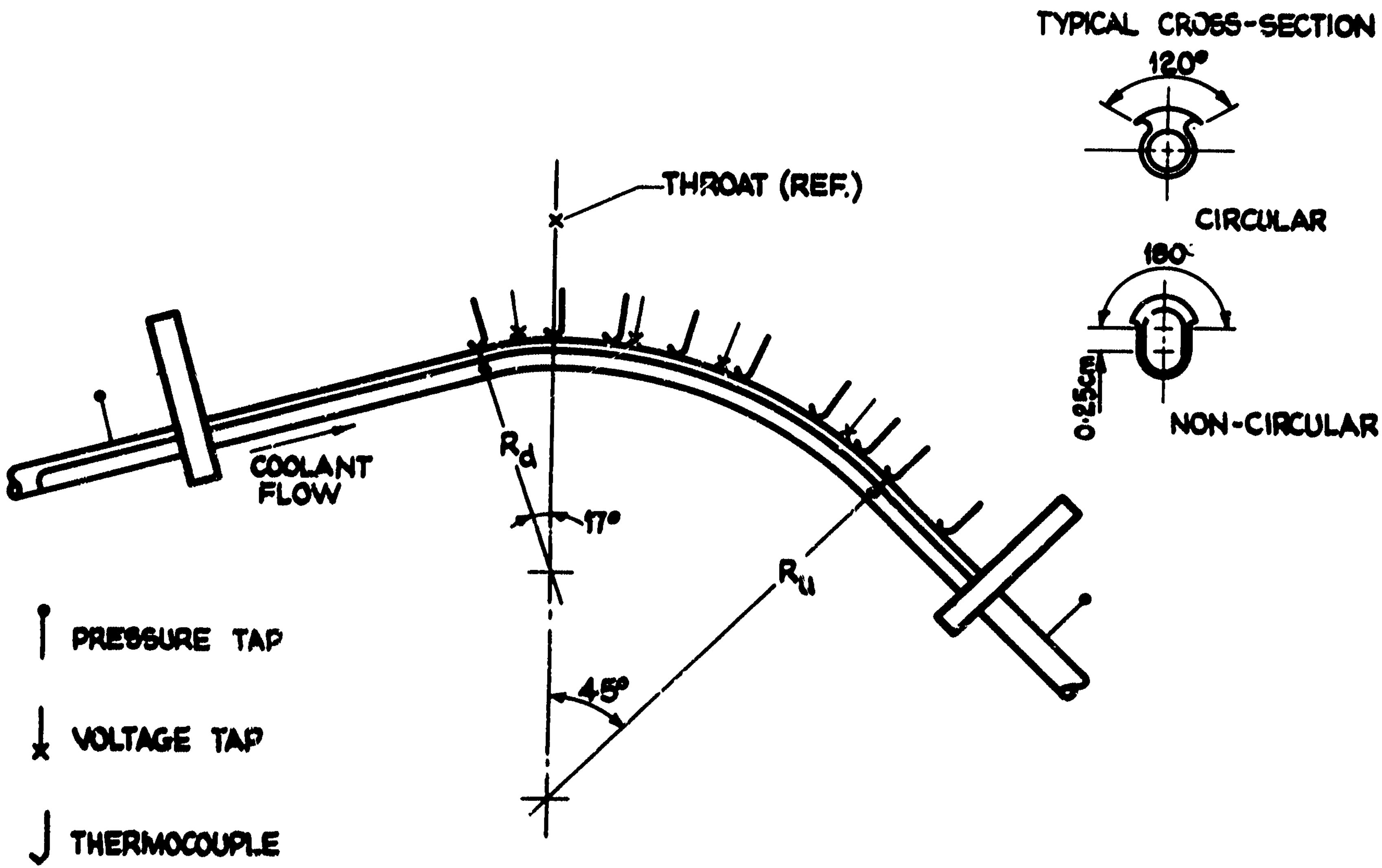

FIG. 5 SCHEMATIC DIAGRAM OF CURVED TUBE TEST SECTIONS (REF. 37)

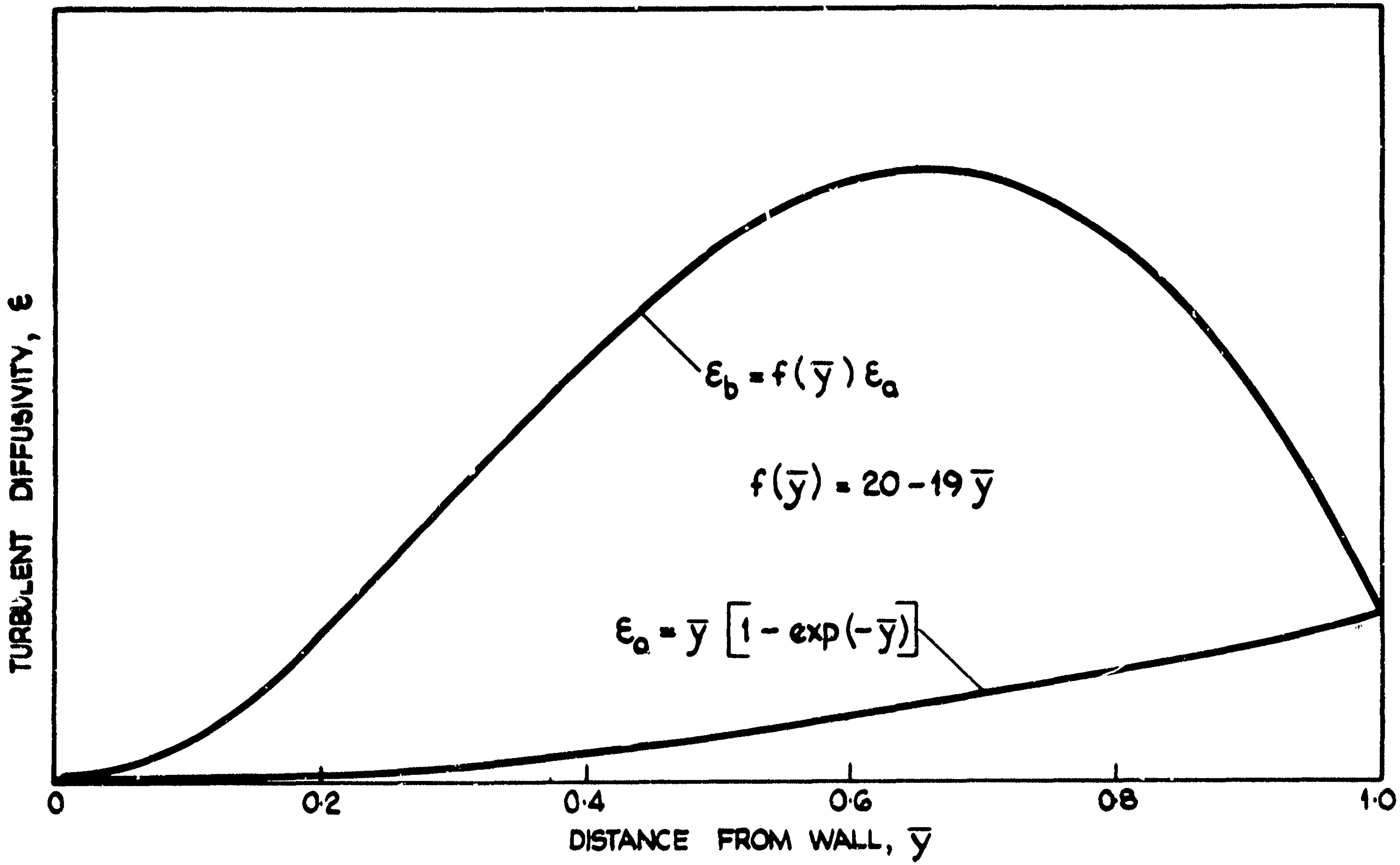

FIG.6 DISTRIBUTIONS OF TURBULENT DIFFUSIVITY IN THE LAMINAR SUB-LAYER.